Nuclear Materials and Energy 9 (2016) 41–45

Contents lists available at ScienceDirect

Nuclear Materials and Energy

journal homepage: www.elsevier.com/locate/nme

High heat flux testing of first wall mock-ups with and without neutron irradiation

G. Pintsuk[a,*], B. Bellin[b], A. Gervash[c], J. Linke[a], N. Litunovsky[c], P. Lorenzetto[b]

[a] Forschungszentrum Jülich, 52425 Jülich, Germany
[b] Fusion for Energy, 08019 Barcelona, Spain
[c] Efremov Institute, St. Petersburg 196641, Russia

ARTICLE INFO

Article history:
Received 20 November 2015
Revised 9 February 2016
Accepted 13 February 2016
Available online 6 April 2016

Keywords:
First wall
Beryllium components
Neutron irradiation
High heat flux testing

ABSTRACT

Beryllium as the plasma facing material for the first wall of ITER will be exposed to thermal, particle and neutron loads. In the frame of the European qualification program for ITER, two HIPped beryllium small scale flat-tile mock-ups consisting of a steel support structure, a CuCrZr/Cu heat sink and two beryllium tiles on top were manufactured by CEA. One mock-up was exposed to neutron irradiation up to 0.75 dpa in beryllium in the RBT-6 fission reactor at Dimitrovgrad, Russia, while the other one was kept as reference. Furthermore, an identical mock-up was produced in Russia by manufacturing via electron beam induced rapid brazing and also exposed to the same neutron irradiation conditions.

For qualification, all three flat-tile mock-ups were exposed to cyclic steady state heat loads in the electron beam facility JUDITH-1 up to a maximum of 3.0 MW/m^2. Thereby, each tile was loaded individually as the full loading area exceeds the limits of the facility.

1. Introduction

The first wall and divertor of ITER will be exposed to high thermal, particle and neutron loads [1]. In dependence on the location in the main chamber, the material and components have to accommodate heat fluxes from 2 MW/m^2 (normal heat flux) to 4.7 MW/m^2 (enhanced heat flux) [2]. For the first wall, beryllium with all its advantageous and disadvantageous properties is chosen as plasma facing material as optimum solution with regard to plasma power handling and particle flux characteristics [3]. Thereby, the development of first wall plasma facing components is already in the qualification phase, which is done by high heat flux testing [4]. As part of the European beryllium qualification program for the use as plasma facing material on first wall components for ITER [5], two HIPped beryllium small scale flat-tile mock-ups with the normal heat flux design were manufactured by CEA [6]. The mock-ups consist of a stainless steel support structure, a CuCrZr/Cu heat sink and two beryllium tiles on top. Furthermore, an identical mock-up was produced by Efremov, Russia, by manufacturing via fast brazing [7].

The aim was to investigate synergistic effects of neutron and thermal loads in subsequent testing campaigns. Accordingly, one European mock-up and the Russian mock-up were exposed first to neutron irradiation up to 0.75 dpa in the RBT-6 fission reactor at Dimitrovgrad, Russia, while the other one was kept as reference [8]. Secondly, for qualification, all three small-scale flat-tile mock-ups were exposed to cyclic steady state heat loads in the electron beam facility JUDITH-1 at Forschungszentrum Juelich starting from screening tests at 0.5 MW/m^2 up to a maximum of 200 cycles at 3.0 MW/m^2. In total up to 1700 cycles at different power densities were applied with a maximum of 500 cycles at a particular power density. Thereby, each tile was loaded individually as the full loading area would have exceeded the limits of the facility.

Qualification criteria are not only the number of sustained cycles but also the beryllium surface temperature at a respective power density and, if existing, the failure mode.

2. Components, irradiation and testing conditions

Each of the three investigated mock-ups consists of 2 identical beryllium tiles with dimensions of $\sim 56 \times 56 \times 9\,mm^3$ and $\sim 56 \times 56 \times 10\,mm^3$ for the European mock-ups and the Russian mock-up, respectively, and a gap of 2 mm between these tiles. For the European mock-ups and the Russian mock-up the beryllium grades S65-C and TGP-56 were used, respectively. The tiles are

* Corresponding author.
E-mail address: g.pintsuk@fz-juelich.de (G. Pintsuk).

http://dx.doi.org/10.1016/j.nme.2016.02.003

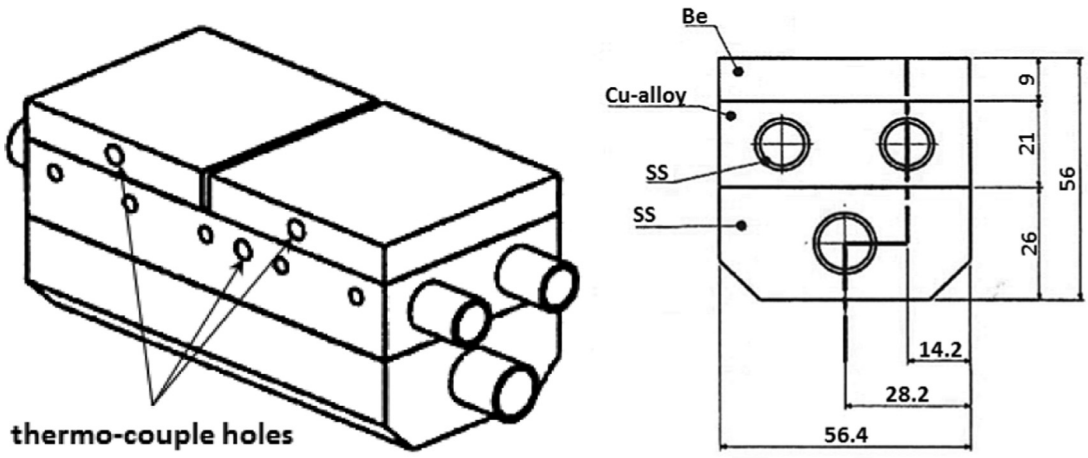

Fig. 1. Overview and cross section of the European Be mock-up including main dimensions.

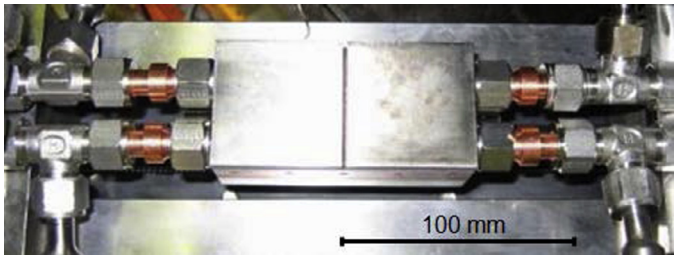

Fig. 2. Installation of the Be mock-ups in JUDITH-1 by the specially developed clamping device also for handling via manipulators.

HIPped to a 21 mm high CuCrZr heat sink containing two symmetrically positioned stainless steel cooling channels with 10 mm inner diameter and 1 mm wall thickness. As supporting structure a 26 mm stainless steel back plate is joined to CuCrZr. This support structure contains an additional cooling tube of 12 mm inner diameter (Fig. 1).

Neutron irradiation of one European mock-up and the Russian mock-up was performed in the RBT-6 reactor at Dimitrovgrad. In-pile thermal cycling (3720 thermal cycles at 60 °C coolant temperature and a surface heat flux of 0.5 MW/m^2) of the mock-ups was performed to a damage level of 0.11 dpa (Be) / 0.15 dpa (CuCrZr and SS). This was followed by irradiation in the non-cycling regime up to an average fluence of fast neutrons ($E > 0.1$ MeV) of 1.4×10^{21} n/cm^2 still at 60 °C coolant temperature. This resulted for Be and CuCrZr/stainless steel in a volume averaged damage level of 0.75 ± 0.05 dpa and 1.05 ± 0.05 dpa, respectively. For the thermal monitoring during neutron irradiation, thermo-couple holes were inserted at the side of the component in beryllium and CuCrZr (Fig. 1).

The high heat flux (HHF) testing was done at the electron beam facility JUDITH-1 at Forschungszentrum Juelich, which is located in a hot cell [9]. For the installation of the irradiated mock-ups and the required remote handling via manipulators, a new clamping device was developed (Fig. 2). The connection between cooling circuit and mock-up was established via conical adaptors made from pure Cu. Thereby, due to the limited manageability via manipulators, cooling was only performed via the two stainless steel cooling tubes in CuCrZr while the stainless steel support structure had to be left uncooled. However, based on experience the influence of cooling the stainless steel support structure on the overall temperature field was assumed to be marginal.

Table 1
High heat flux testing parameters in JUDITH-1.

$A_{loading}$	~56 × 56 mm^2
Scanning frequency	40 × 31 kHz
v (water)	~2.8 m/s
p_{in} (water)	~0.4 MPa
T_{in} (water)	RT
t @ cycling	50 / 50 s

Table 2
Planned loading conditions for the qualification of the mock-ups.

# of cycles	P [MW/m^2]
500	1.8
500	2.4
500	2.75
200	3.0
200	3.25, 3.5, 3.75, …

Each tile (A and B) was loaded individually as the full loading area would have exceeded the limits of the facility. Furthermore, the electron beam has a beam diameter at full width half maximum of 1 mm, requiring high frequency scanning across the surface in a triangular scanning mode. The chosen frequencies and all other parameters are shown in Table 1. Thereby, for the cooling circuit of JUDITH-1 a linear dependence of water velocity and pressure exists resulting in a relatively low inlet pressure due to the required low flow rate of ~2.8 m/s. The chosen cycling time of 50 s on and 50 s off allows the component to reach steady state in the loading but also in the cooling regime.

For allowing the qualification of the component in a first step the initial performance of the mock-ups and in particular the joints was investigated by various screening cycles from 0.5 to 1.8 MW/m^2. In a second step, several cycling steps were performed applying up to 500 cycles at a particular loading condition (Table 2) until failure of the component occurred or the temperature limit of the facility, i.e. 700 °C, was reached.

3. Results and discussion

During HHF-testing of the non-irradiated European mock-up, both tiles, although loaded individually, started overheating at one outer corner of the loaded area (Fig. 3) during cycling at 2.75 MW/m^2. However, even up to 200 cycles at 3 MW/m^2 the tiles

Table 3
Comparison of fatigue resistance and failure modes of reference and irradiated mock-ups.

	Tile A	Tile B
EU – non-irr.	157 cycles @ 3.0 MW/m^2: stop due to exceeding of temperature threshold; continuous degradation by overheating of one corner that started during cycling at 2.75 MW/m^2	200 cycles @ 3.0 MW/m^2 and screening @ 3.25 MW/m^2: stop due to exceeding of temperature threshold; continuous degradation by overheating of one corner that started during cycling at 2.75 MW/m^2
EU – irr.	11 cycles @ 3.0 MW/m^2: stop due to spontaneous failure	500 cycles @ 2.4 MW/m^2 and screening @ 2.75 MW/m^2: stop due to local exceeding of temperature threshold caused by local melting during cycling at 1.8 MW/m^2 due to facility malfunction
Russia – irr.	25 cycles @ 2.4 MW/m^2: stop due to spontaneous failure	500 cycles @ 1.8 MW/m^2 and screening @ 2.1 MW/m^2: stop due to spontaneous failure

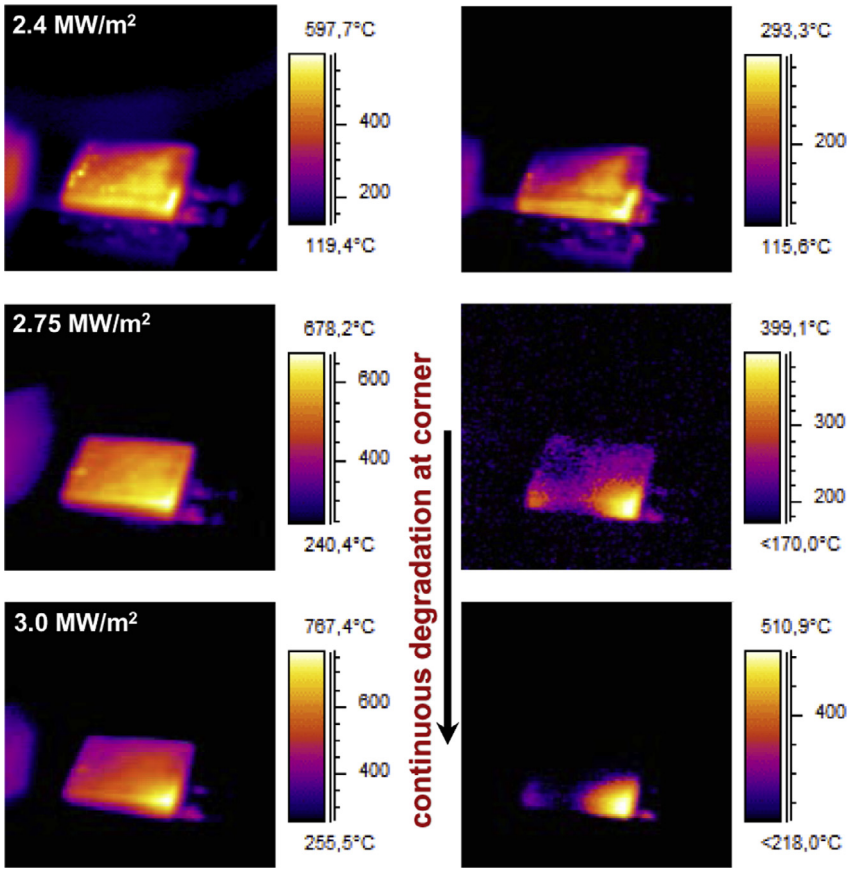

Fig. 3. IR-images of the non-irradiated European mock-up, tile A, at the end of the screening at the particular power density after cycling (left) and after 5 s cool down (right).

are still attached and the tests were stopped due to exceeding the allowed surface temperature in JUDITH-1 in the overheated area (Table 3).

In contrast, the irradiated European mock-up failed abruptly at the edge between the two Be tiles. For tile A this occurred after 11 cycles at 3.0 MW/m^2 without showing any sign of degradation before failure (Fig. 4). For tile B a malfunction of the facility's deflection system occurring during cycling at 1.8 MW/m^2 caused local melting of the surface. Based thereon, the tests on tile B were stopped after screening at 2.75 MW/m^2 due to exceeding the facility's temperature threshold at the affected molten area (Table 3). However, despite this local overheating, the cool down performance of tile B did not show any degradation of the heat removal capability up to this loading step.

Similar to the irradiated European mock-up, the Russian mock-up failed abruptly on both tiles (Table 3). Thereby, the sustained loading conditions are a maximum of 25 cycles at 2.4 MW/m^2. In both cases a full detachment of the Be-tile occurred. Thereby, the crack first runs along the Be/Cu interface while it then proceeds into the Be-tile creating a hemisphere like structure (Fig. 5a). Although the irradiated European mock-up did not detach completely, in a side view (Fig. 5b) similarly partial detachment at the Be/Cu interface and crack formation into Be was found for both tiles. A possible reason for the change in failure mode after neutron irradiation is the neutron induced embrittlement and reduced ductility of beryllium [3,10].

The comparison of the reference and irradiated European mock-up shows that the measured surface temperatures after neutron irradiation are significantly higher (Fig. 6). Thereby, it needs to be noted that due to the lack of a calibration tile and no measured temperature by the two color pyrometer (range: 550–1600 °C) the surface emissivity was set for the Russian mock-up and the non-irradiated European mock-up, based on former experience, to an emissivity of 0.3. A change of the emissivity for the non-irradiated European mock-up between cycling of tile A at 2.4 MW/m^2 and 2.75 MW/m^2, attributed to slight air ingress during testing and a

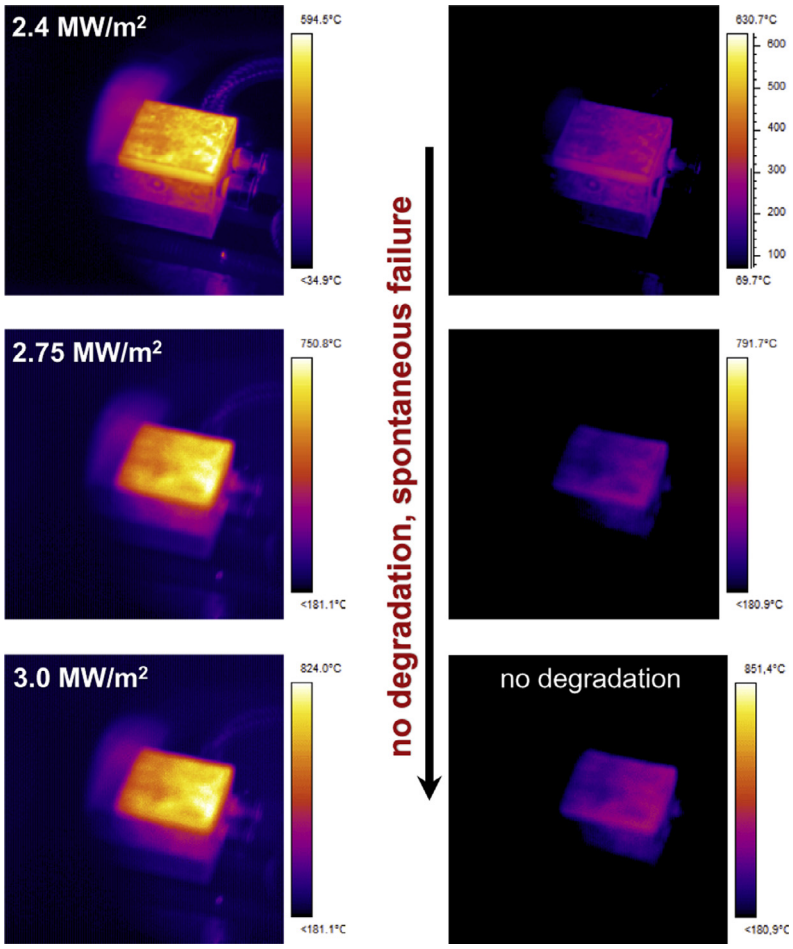

Fig. 4. IR-images of the irradiated European mock-up, tile A, at the end of the screening at the particular power density after cycling (left) and after 5 s cool down (right).

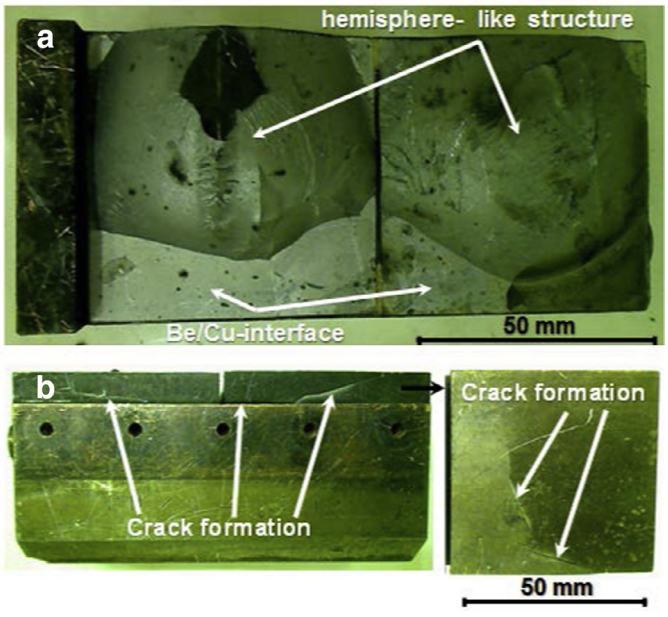

Fig. 5. Macroscopic image of the loaded irradiated mock-ups; (a) Russian mock-up with detached tiles; (b) European mock-up showing crack formation at the Be/Cu interface and in Be.

machine shut down for a longer period leading to the formation of a surface oxidation layer, has been identified as the most probable reason for the measured temperature increase shown in Fig. 6. For the irradiated European mock-up a calibration via two-color pyrometer was possible resulting in an emissivity of 0.39. On the one hand the higher temperatures after irradiation might be attributed to the degradation of the thermo-physical properties of the materials, which experimentally only occurs for low irradiation temperature and high dose [3] and therefore would correspond to the applied irradiation conditions at 60 °C. On the other hand, due to the applied in-pile cyclic loading at 0.5 MW/m^2 also a degradation at the joined interfaces could have occurred. Neither thermo-physical nor metallographic analyses could be performed to verify one or both hypotheses. The discrepancy in surface temperature between the irradiated European and Russian mock-up is to a large extent a result of the increased thickness of the Be-tile by 1 mm in combination with the used different surface emissivity values. The use of different Be-grades for the European and Russian mock-ups might also play a minor role. However, based on the limited number of tests and the failure mode shown in Fig. 5, from the results a superiority of one or the other joining technology cannot be deduced. Occurring differences in power handling capability might be attributed to the thickness and the material properties of the used Be-grades.

Despite the significant difference in temperature, the change in overall performance before and after neutron irradiation is comparably low and at least thermal fatigue loading up to 500 cycles at 2.75 MW/m^2 was sustained by the European mock-up in

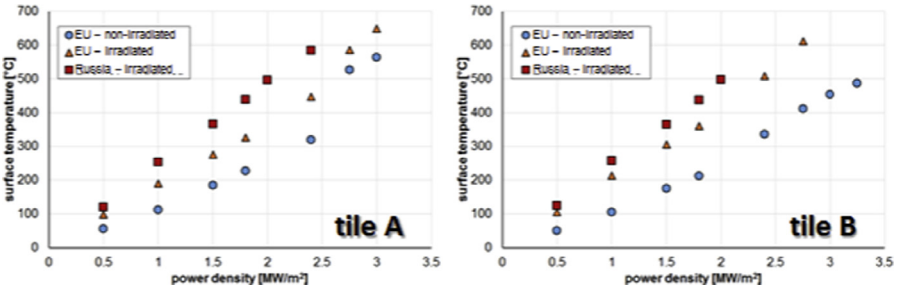

Fig. 6. Temperature evolution for all three investigated mock-ups during screening at the particular power density for tile A and B.

all cases (a clear statement about the performance of tile B of the irradiated European mock-up is not possible due to mentioned reasons, Table 3). However, the abrupt failure mode after neutron irradiation makes it difficult to detect failures well before they become critical.

4. Summary

As part of the European beryllium qualification program for the use as plasma facing material on first wall components for ITER, two HIPped beryllium small scale flat-tile European mock-ups produced by CEA and an identical Russian mock-up produced by Efremov were neutron irradiated up to 0.75 dpa and subsequently high heat flux tested. The obtained findings can be summarized as follows:

- Neutron irradiation influences the thermal performance by increasing the measured surface temperature; this could be caused either by (a) a decreasing thermal conductivity of the plasma facing and heat sink materials or (b) a degradation at the joined interface between beryllium and copper.
- Location and mode of failure changed from (a) a slowly developing delamination at an outer corner without neutron irradiation to (b) an abrupt failure starting at the edge between two tiles for the neutron irradiated mock-ups; possible reason for this change is neutron induced embrittlement of beryllium.
- Neutron induced embrittlement may also trigger the detachment of neutron irradiated beryllium tiles, which started by cracking at the Be/Cu interface followed by crack deflection into beryllium.

Acknowledgment

The work leading to this publication has been funded partially by Fusion for Energy/EFDA under Grant TW4-TVB-HFTEST. This publication reflects the views only of the authors, and Fusion for Energy cannot be held responsible for any use which may be made of the information contained therein.

References

[1] R.A. Pitts, S. Carpentier, F. Escourbiac, T. Hirai, V. Komarov, A.S. Kukushkin, S. Lisgo, A. Loarte, M. Merola, R. Mitteau, A.R. Raffray, M. Shimada, P.C. Stangeby, J. Nucl. Mater. 415 (2011) S957–S964.
[2] R. Mitteau, B. Calcagno, P. Chappuis, R. Eaton, S. Gicquel, J. Chen, A. Labusov, A. Martzin, M. Merola, R. Raffray, M. Ulrickson, F. Zacchia, Fusion Eng. Des. 88 (2013) 568–570.
[3] G. Federici, R. Doerner, P. Lorenzetto, V. Barabash, Compr. Nucl. Mater. 4 (2012) 621–666 Chapter 4.19.
[4] R. Mitteau, R. Eaton, G. Perez, F. Zacchia, S. Banetta, B. Bellin, A. Gervash, D. Glazunov, J. Chen, Fusion Eng. Des. 98–99 (2015) 1367–1370.
[5] S. Banetta, B. Bellin, P. Lorenzetto, F. Zacchia, B. Boireau, I. Bobin, P. Boiffard, A. Cottin, P. Nogue, R. Mitteau, R. Eaton, R. Raffray, A. Bürger, J. Du, J. Linke, G. Pintsuk, T. Weber, Fusion Eng. Des. 98–99 (2015) 1211–1215.
[6] P. Lorenzetto, B. Boireau, C. Boudot, Ph. Bucci, P.E. Frayssines, A. Furmanek, P. Hajeke, O. Gillia, A. Peacock, I. Ricapito, M. Roedig, P. Sherlock, F. Schmalz, S. Tähtinen, Fusion Eng. Des. 83 (2008) 1015–1019.
[7] I.V. Mazul, V.A. Belyakov, R.N. Giniatulin, A.A. Gervash, V.E. Kuznetsov, A.N. Makhankov, V.S. Sizenev, Fusion Eng. Des. 86 (2011) 576–579.
[8] N. Litunovsky, A. Gervash, P. Lorenzetto, I. Mazul, R. Melder, J. Nucl. Mater. 386-388 (2009) 979–982.
[9] R. Duwe, W. Kuehnlein, H. Muenstermann, Fusion Technol. (1995) 355–358.
[10] L.L. Snead, J. Nucl. Mater. 326 (2004) 114–124.